Quantum Hall criticality, superconductor-insulator transition, and quantum percolation

Yonatan Dubi,[1] Yigal Meir,[1,2] and Yshai Avishai[1,2]
[1]*Physics Department, Ben-Gurion University, Beer Sheva, 84105, Israel*
[2]*The Ilse Katz Center for Meso- and Nano-scale Science and Technology, Ben-Gurion University, Beer Sheva, 84105, Israel*
(Received 19 November 2004; published 15 March 2005)

A model consisting of a mixture of superconducting and quantum links is proposed to describe the integer quantum Hall transition. The quantum links correspond to tunneling of electrons between trajectories trapped in adjacent potential valleys, while the superconducting links mimic the merging of these trajectories once the Fermi energy exceeds the saddle point energy separating the two valleys. The quantum Hall transition in this model corresponds to percolation of the superconducting links. Numerical calculations and scaling analysis using two different approaches yield the critical exponent $\nu \approx 2.4$ and a two-peak conductance distribution at the critical point. The role of quantum coherence is discussed, allowing an interpretation of $\nu \approx 1.3$, found in some experiments, in terms of the percolation critical exponent. The model suggests that the critical behavior of the superconductor-insulator transition (on the insulating side) is in the same universality class as the quantum Hall transition.

DOI: 10.1103/PhysRevB.71.125311 PACS number(s): 73.43.Nq, 71.30.+h, 74.20.Mn

The integer quantum Hall (QH) effect is one of the most studied manifestations of a second order quantum phase transition.[1] As such it is characterized by a length scale ξ, which controls the decay of wave functions (and conductance) with system size and diverges at a critical point with a universal power (critical exponent) ν. Most numerical investigations in various models yield $\nu \simeq 2.4$.[2] Experiments, however, disagree on the critical behavior. While some indeed yield an exponent close to the theoretical prediction,[3] others yield an exponent $\nu \simeq 1.3$, close to the classical percolation critical exponent, $\nu_p = 4/3$.[4] This points toward the important role of percolation in the QH transition (QHT), as has been indeed experimentally demonstrated.[5] At the same time, other experiments claim that there is no critical behavior at all.[6]

A similar lack of clarity prevails with the critical exponent describing the two-dimensional superconducting-insulator transition (SIT), which can be induced either by a continuous change of film thickness or by a magnetic field. While some experiments (on the insulating side) report an exponent $\nu \simeq 1.3$, (Ref. 7) others yield $\nu \simeq 2.8$ (Ref. 8). On the superconducting side only the value $\nu \simeq 1.4$ has been reported.[8] Similar to the QH case, some experiments present evidence that there is no critical behavior at all.[9] The relevance of the percolation of superconducting islands to the SIT has been pointed out as well[10] and has been experimentally substantiated both in granular[11] and in amorphous systems.[12] Recent scanning tunneling measurements[13] have directly demonstrated the separation of these systems into superconducting areas and metallic or insulating ones.

In this work we develop a model to describe the QHT with direct relation to SIT and to quantum percolation. It enables us to clarify the interplay of classical percolation with quantum tunneling and interference in describing the critical behavior of the QHT. In addition to providing an estimate of the critical exponent and the fixed-point conductance distribution at the critical point, it explains the appearance (in some experiments) of the critical exponent associated with classical percolation in the QHT (Ref. 4). Further analysis leads us to conjecture that, as viewed from the insulating side, the SIT belongs to the same universality class as the QHT, thereby explaining why theoretical and experimental estimates yield similar exponents for the two seemingly distinct transitions.

The model is based on the following picture. In strong magnetic fields, electrons with Fermi energy ϵ_F perform small oscillations around equipotential lines. When ϵ_F is small, their trajectories are trapped inside potential valleys, with weak quantum tunneling occurring between adjacent valleys. We associate each such potential valley with a site in a lattice. Nearest neighbor valleys (trapped orbits) are connected by links representing random tunneling between them (see Fig. 1). As ϵ_F increases and crosses the saddle-point energy separating two neighboring valleys, the two isolated trajectories coalesce, the electron can freely move from one valley to its neighbor, and the link connecting them becomes perfect or "superconducting" (SC). Here the phrase superconducting refers purely to perfect transmission. The QHT occurs when there is an "infinite" cluster of SC links connecting the two sides of the system. The critical behavior is determined by quantum mechanical transport of an electron from one side of the system to the other, namely, tunneling and interference. The main difference between the present model and previous models is the emergence of two length scales, the localization length and the percolation coherence length, both diverging at the critical point. The interplay of these scales with system size may lead to different apparent critical behaviors. Additionally, unlike, e.g., the Chalker-Coddington (CC) model,[14] where the random phases are the only source of randomness, here the randomness emerges from the energy distribution (see below). This allows us to study the effect of interference on the critical behavior.

The saddle points, which are mapped onto links in the lattice, have random energies ϵ_i, sampled from some distribution $G(\epsilon_i)$. The transmission of electrons at energy ϵ_F through a link at energy $\epsilon_i > \epsilon_F$ is given by

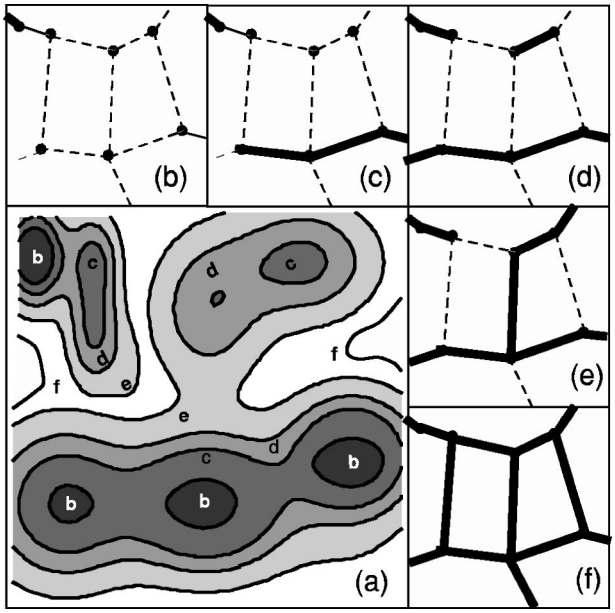

FIG. 1. Mapping of the quantum Hall system onto a lattice model. (a) Equipotential lines for five different Fermi energies. At low ϵ_F electron trajectories are confined to potential valleys. Each such valley is denoted by a point in the discrete model (b)–(f). In order to move from one such valley to another, the electron has to tunnel through a saddle point—dotted links in (b)–(f). As ϵ_F exceeds the saddle-point energy these valleys are joined and the electron can move perfectly from one valley to another—solid links in (b)–(f). Figures (b)–(f) correspond to a system with ϵ_F values up to the equipotential line marked by the appropriate letter in (a). Note that in (d) the solid links percolate, meaning that at this Fermi energy an electron can traverse the whole system on an equipotential line, corresponding to the quantum Hall transition.

$$T(\epsilon_F) = \exp[-\alpha(\epsilon_i - \epsilon_F)], \tag{1}$$

describing tunneling through a parabolic barrier. For $\epsilon_F > \epsilon_i$, on the other hand, the transmission through the link is perfect [i.e., $T(\epsilon_F)=1$] and the link is considered to be SC. Accordingly, the concentration of SC links is then given by $p(\epsilon_F)=\int_{-\infty}^{\epsilon_F} G(\epsilon)d\epsilon$. Percolation of the SC links (that is, occurrence of the QHT) is associated with diverging localization length or, equivalently, with a length-independent transmission. The critical threshold is model dependent, but the critical exponent is universal. Our attention is then focused on the critical behavior near this phase transition point.[15] For the sake of computational simplicity we deal henceforth with a square lattice.

Two different approaches for implementing this quantum mechanical problem are presented. The first employs a scattering matrix formalism. Each link in the lattice carries two edge states from neighboring valleys, moving in opposite direction. [see Fig. 2(a)]. The scattering matrix for each link is characterized by complex transmission and reflection amplitudes associated with electron tunneling between adjacent valleys. The tunneling probability is determined as follows: for each link, a saddle-point energy ϵ_i is randomly chosen from a uniform distribution $G(\epsilon_i)$ on $[-\frac{1}{2},\frac{1}{2}]$. If $\epsilon_F > \epsilon_i$, then

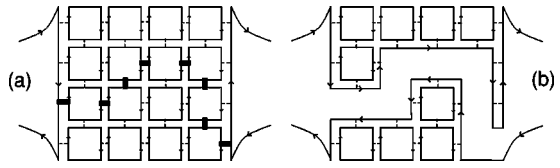

FIG. 2. The scattering matrix approach: each link carries two counterpropagating edge modes (a). A nonzero transmission (broken lines) allows electrons to tunnel between adjacent sites (potential valleys). When the transmission is unity [bold lines in (a)], these two valleys merge, and an edge state can freely propagate from one to another. A percolation of these perfect transmission links (b) correspond to an edge state propagating through the system without backscattering.

$T=1$, otherwise the transmission probability through the link is given by Eq. (1). The allowed phases of the matrix elements are chosen randomly from a uniform distribution between 0 and 2π. For perfect links ($T=1$), the electron follows these edge states from one valley to another. It is easily seen [Fig. 2(b)] that when these percolate, we have two edge states propagating through the system in opposite directions, without scattering between left-going and right-going channels. Consequently, the percolation point corresponds to the QHT.

We evaluate the logarithm-averaged transmission $\bar{T}(L) \equiv \exp(\langle \log T \rangle)$, through a system of the geometry depicted in Fig. 2, of linear sizes $L=10,15,\ldots,50$, averaged over 5000 realizations, for different values of ϵ_F near the critical point. Figure 3 displays the raw data. In (a) we plot the dependence of the transmission on ϵ_F (in terms of prob-

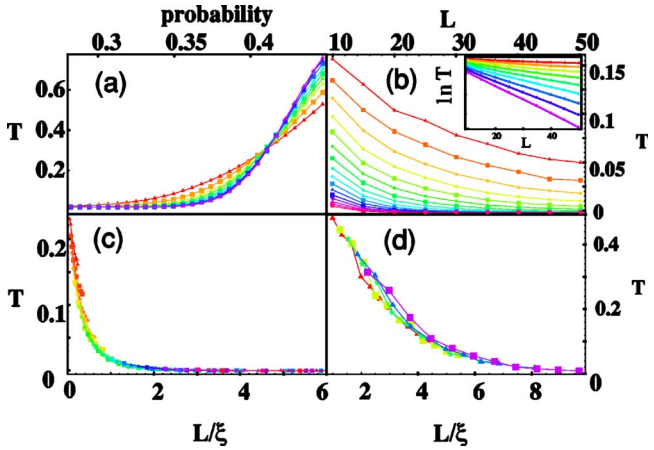

FIG. 3. (Color online) Numerical results of the scattering matrix approach for $\alpha=12$ [See Eq. (1)]. (a) The logarithm-averaged transmission coefficient $\bar{T}$ as a function of ϵ_F for system lengths $L=10,\ldots,50$. (b) $\bar{T}$ as a function of L for different concentrations, $p=0.41,0.4,\ldots,0.3$. Inset: the same data on a semi logarithmic plot demonstrating an $\exp[-L/\bar{\xi}(\epsilon_F)]$ dependence of the transmission. (c) The raw data curves for $\bar{T}$ [Fig. 3(b)] are collapsed onto a single curve by scaling each curve by an energy-dependent localization length, diverging at the critical energy with an exponent 2.34 ± 0.10. (d) Scaling of the data obtained by the tight-binding approach. For energies $\epsilon=-0.050,-0.055,\ldots,-0.1$ the data collapse yields the exponent $\nu=2.43\pm0.1$.

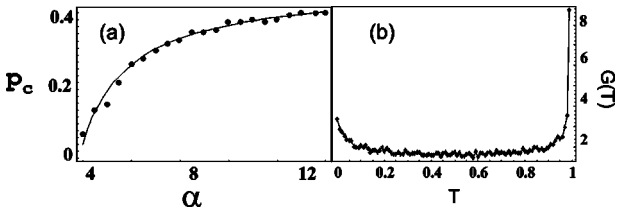

FIG. 4. (a) The dependence of the critical point on the parameter α in Eq. (1). Bold points are raw data and the solid line is the analytic curve. (See text.) (b) The fixed distribution of T at the critical point, calculated using the scattering-matrix approach.

ability of SC links) for different sizes. The existence of a critical point, where the curves cross and the transmission is independent of length, is evident. In (b) we show the dependence of the transmission on length for different concentrations. The inset depicts the log of the transmission as a function of length. The straight lines demonstrate that indeed, $\overline{T(L)} \propto \exp[-L/\xi(\epsilon_F)]$. All these curves coalesce [Fig. 3(c)], after scaling the system length by the energy-dependent localization length $\xi(\epsilon_F)$. $\xi(\epsilon_F)$ is found to diverge at the critical point with an exponent 2.34 ± 0.1, in agreement with previous numerical approaches. The exponent ν is found to be independent of the value of α in Eq. (1). The critical probability, i.e., the probability (or Fermi energy) at which the transmission is length independent, on the other hand, does depend on α. This dependence can be understood as follows: The transmission through the system at the critical point, T_0, is independent of length and of the value of α and is given by an average over the fixed point distribution [Fig. 4(b)]. The critical Fermi energy for a given $\alpha, \epsilon_c(\alpha)$, is determined by the value of ϵ_F at which the transmission becomes equal to T_0. One then finds $\epsilon_c(\alpha) = \log(T_0)/\alpha$ [Eq. (1)], or $p_c(\alpha) = \frac{1}{2} + \log(T_0)/\alpha$. This function agrees excellently with our numerical data [see Fig. 4(a)], with a fitting parameter $T_0 = 0.4$, in rough agreement with the value $T_0 = 0.32$, obtained by logarithm averaging the fixed distribution at the critical point. Figure 4(b) displays the distribution of transmissions at the critical point. The double peak structure agrees with previous numerical calculations for the integer QHT.[16]

To complement the above study, we develop a second approach, employing a tight-binding Hamiltonian

$$\mathcal{H} = \sum_{\langle i,j \rangle} v_{ij} c_i^\dagger c_j + \text{H.c.} \tag{2}$$

Determination of the parameters v_{ij} follows the procedure described above for determining the scattering matrix parameters. We associate a random saddle-point energy ϵ_{ij} with each link joining lattice sites i and j. When $\epsilon_{ij} > \epsilon_F$ the hopping matrix element v_{ij} for that link is chosen such that it will give the transmission coefficient (1). When $\epsilon_{ij} < \epsilon_F$ the link is considered perfect, or SC. When two sites are joined by such an SC link, they are merged into a single site. This guarantees that only when the SC links percolate, the conductance of the system will not decay with length, so that p_c will be independent of α. The conductance is now calculated numerically, by attaching a single-channel wire to both sides

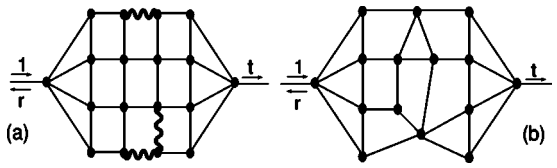

FIG. 5. The tight-binding approach—sites connected by SC links [wiggly lines in (a)] are merged into a single site and then the transmission of the modified lattice (b) is calculated using the tight-binding Hamiltonian (2).

of the lattice, and calculating the transmission through the system for an electron at the Fermi energy. This calculation involves two stages (see Fig. 5): (a) identifying clusters of sites connected by SC links as a single site, and (b) calculating T by solving the tight-binding equations in the reduced space.[17]

Data are generated for lattice length $L = 6, 10, \ldots, 34$, and averaged over 1500 realizations. Following the same scaling procedure as described above, the curves collapse onto a single curve, a procedure that yields the critical exponent $\nu = 2.43 \pm 0.1$ [Fig. 3(d)]. We also calculate the conductance distribution at the critical point and find that it shows a two-peak structure, similar to that of the S-matrix approach. Both the critical exponent and the critical point, $p_c = 1/2$ are independent of the parameter α, for a broad range of values.[18]

We also checked the dependence of the critical exponent ν for different functional forms of the tunneling probability $T(\epsilon)$ in addition to that described by Eq. (1). The functional form suggested by Fertig and Halperin,[19] $T = 2/\{1 + \exp \times [-\pi(\epsilon_i - \epsilon_F)]\}$, yields very similar results, with a value $\nu = 2.49 \pm 0.1$. A similar value is obtained when the link transmission coefficients are taken from a uniform distribution. Thus, the physics does not depend on the exact functional form of $T(\epsilon)$ or on its distribution. The change in the critical exponent from its classical value can be traced to the fact that as ϵ_F, or $p(\epsilon_F)$ are varied, the transmission amplitude through the quantum insulator is modified as the bottle-neck link changes. We also note that repeating the same calculations without random phases does not yield any reasonable scaling of the data. Thus interference effects are crucial in obtaining the correct critical behavior.

If one tries to employ the scaling analysis described above, including energies that are not too close to the critical one, the collapse of the data becomes worse and in fact can be better fitted with the classical exponent $\nu = 4/3$ [Figs. 6(a) and 6(b)]. This is consistent with the above picture as the difference between the classical and the quantum exponents arise due to the additional dependence of the tunneling amplitude on $\epsilon - \epsilon_c$, a dependence that becomes less relevant away from the critical point. In other words, the system size becomes smaller than the localization length, but is still larger than the percolation coherence length, and the critical behavior of the latter dominates. This observation may also explain why some experiments report a classical percolation exponent for the QHT (Ref. 4).

So far the term "SC links" was used to describe perfect links in the QH regime. The model, however, suggests a further correspondence between the QH critical

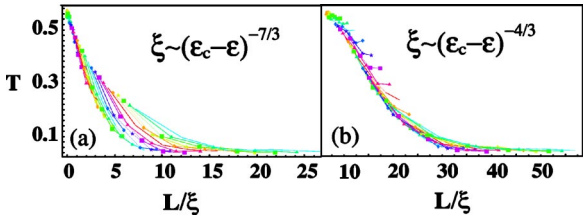

FIG. 6. (Color online) (a) Same as in Fig. 3(d), including a larger range of energies $\epsilon=-0.01,-0.02,\ldots,-0.2$. These data can be better fitted with an exponent $\nu=4/3$ (b).

behavior and the critical behavior of the SC-insulator transition on the insulating side. In the latter case the conductance is dominated by the nonsuperconducting regions. Superconductivity-related effects, such as Josephson coupling between different islands and the proximity effect, define the extent and the geometry of the SC regions, and, consequently, that of the non-SC ones. Classical percolation has already been invoked in this context to explain the observed critical exponent $\nu\simeq 1.3$.[7] Here we claim that the quantum coherent processes may explain the experimental observations of $\nu\simeq 2.8$. The relation between the critical behavior and two competing length scales, namely the SC coherence length and the localization length, has been demonstrated experimentally.[20] Moreover, the SIT is not symmetric around the critical point, which is similar to the model described here. In addition, this relation between these two apparently different transitions also explains the fact that the critical resistance observed at the SIT seems to be distributed around values somewhat larger than $h/4e^2$, expected from duality.[21] This relation can be further investigated experimentally by studying the full resistance distribution at the SI threshold, as do such experiments for the QHT.[22] We predict a two-peak structure, as for the QH transition. The similarity of the QHT and the SIT has already been pointed out in Ref. 23, which emphasized the noncritical behavior and the role of decoherence. In fact, the model introduced in this work allows the introduction of dephasing in a straightforward way, by attaching current-conserving, phase-breaking reservoirs to some fraction of the links.[24] The interplay between dephasing and classical-quantum crossover will be explored in a future paper.[25]

We acknowledge fruitful discussions with A. Aharony and O. Entin-Wohlman. This research has been funded by the ISF.

[1] For a review see, e.g., *The Quantum Hall Effect*, edited by R. E. Prange and S. M. Girvin (Springer-Verlag, New York, 1990).
[2] B. Huckestein, Rev. Mod. Phys. **67**, 357 (1995).
[3] H. P. Wei, D. C. Tsui, M. A. Paalanen, and A. M. M. Pruisken, Phys. Rev. Lett. **61**, 1294 (1988); S. Koch, R. J. Haug, K. v. Klitzing, and K. Ploog, *ibid.* **67**, 883 (1991); J. F. Hughes, J. T. Nicholls, J. E. F. Frost, E. H. Linfield, M. Pepper, C. J. B. Ford, D. A. Ritchie, G. A. C. Jones, E. Kogan, and M. Kaveh, J. Phys.: Condens. Matter **6** 4763 (1994); F. Hohls, U. Zeitler, R. J. Haug, R. Meisels, K. Dybko, and F. Kuchar, Phys. Rev. Lett. **89**, 276801 (2002).
[4] A. A. Shashkin, V. T. Dolgopolov, and G. V. Kravchenko, Phys. Rev. B **49**, 14 486 (1994); R. B. Dunford, N. Griffin, P. J. Phillips, and T. E. Whall, Physica B, **289** 496 (2001).
[5] I. V. Kukushkin, V. I. Fal'ko, R. J. Haug, K. v. Klitzing, and K. Eberl, Phys. Rev. B **53**, R13260 (1996); A. A. Shashkin, V. T. Dolgopolov, G. V. Kravchenko, M. Wendel, R. Schuster, J. P. Kotthaus, R. J. Haug, K. von Klitzing, K. Ploog, H. Nickel, and W. Schlapp, Phys. Rev. Lett. **73**, 3141 (1994).
[6] D. Shahar, M. Hilke, C. C. Li, D. C. Tsui, S. L. Sondhi, J. E. Cunningham, and M. Razeghi, Solid State Commun. **107**, 19 (1998); N. Q. Balaban, U. Meirav, and I. Bar-Joseph, Phys. Rev. Lett. **81**, 4967 (1998).
[7] D. B. Haviland, Y. Liu, and A. M. Goldman, Phys. Rev. Lett. **62** 2180 (1989); A. F. Hebard and M. A. Paalanen, *ibid.* **65** 927 (1990).
[8] Y. Liu, K. A. McGreer, B. Nease, D. B. Haviland, G. Martinez, J. W. Halley, and A. M. Goldman, Phys. Rev. Lett. **67**, 2068 (1991); A. M. Goldman and Y. Liu, Physica D **83** 163 (1995).
[9] A. Yazdani and A. Kapitulnik, Phys. Rev. Lett. **74**, 3037 (1995); D. Ephron, A. Yazdani, A. Kapitulnik, and M. R. Beasley, *ibid.* **76**, 1529 (1996).
[10] See, e.g., G. Deutscher, Y. Imry, and L. Gunther, Phys. Rev. B **10**, 4598 (1974).
[11] A. Gerber, A. Milner, G. Deutscher, M. Karpovsky, and A. Gladkikh, Phys. Rev. Lett. **78**, 4277 (1997).
[12] D. Kowal and Z. Ovadyahu, Solid State Commun. **90**, 783 (1994).
[13] A. Sharoni, G. Leibovitch, A. Kohen, R. Beck, G. Deutscher, G. Koren, and O. Millo, Europhys. Lett. **62**, 883 (2003); A. Sharoni, I. Asulin, G. Koren, and O. Millo, Phys. Rev. Lett. **92**, 017003 (2004); W. Escoffier, C Chapelier, N. Hadacek, and J-C. Villegier, Phys. Rev. Lett. **93**, 217005 (2004).
[14] J. T. Chalker and P. D. Coddington, J. Phys. C **21**, 2665 (1988).
[15] Our model describes the approach to criticality from one side of the critical point and, by construction, does not display the symmetry of the QHT on the two sides of the transition, in contrast to, e.g., the CC model (Ref. 14).
[16] D. P. Arovas, M. Janssen, and B. Shapiro, Phys. Rev. B **56**, 4751 (1997); A. G. Galstyan and M. E. Raikh, Phys. Rev. B **56**, 1422 (1997); Y. Avishai, Y. Band, and D. Brown, Phys. Rev. B **60**, 8992 (1999).
[17] Y. Meir, A. Aharony, and A. B. Harris, Phys. Rev. Lett. **56**, 976 (1986).
[18] Near $\alpha=0$, the data collapse is worse. At $\alpha=0$ no scaling is observed, and a critical exponent cannot be determined.
[19] H. A. Fertig and B. I. Halperin, Phys. Rev. B **36**, 7969 (1995).
[20] W. Wu and E. Bielejec, cond-mat/0310190 (unpublished).
[21] See, e.g., B. G. Orr, H. M. Jaeger, A. M. Goldman, and C. G. Kuper, Phys. Rev. Lett. **56**, 378 (1986); S. Tayama, M. Honma, and T. Takayama, Phys. Rev. B **43**, 8725 (1990).
[22] D. H. Cobden and E. Kogan, Phys. Rev. B **54**, R17316 (1996).
[23] E. Shmishoni, A. Auerbach, and A. Kapitulnik, Phys. Rev. Lett. **80**, 3352 (1998).
[24] M. Buttiker, Phys. Rev. B **33**, 3020 (1986).
[25] Y. Dubi, Y. Meir, and Y. Avishai, submitted to Phys. Rev. Lett.